Atmosphere. Korean Meteorological Society
Vol. 25, No. 3 (2015) pp. 559-568
http://dx.doi.org/10.14191/Atmos.2015.25.3.559
pISSN 1598-3560 eISSN 2288-3266

연 구 논 문
(Article)

The Fine Power Spectra of the Southern Oscillation Index and Its Components and their Implication

G.-H. Lim[1),*] and Y.-C. Suh[2)]

[1)]*School of Earth and Environmental Sciences, College of Natural Sciences, Seoul National University, Seoul, Korea*
[2)]*Department of Civil Engineering, Pukyong National University, Busan, Korea*

(Manuscript received 5 May 2015; revised 31 July 2015; accepted 3 August 2015)

Abstract As is evident from its definition, Southern Oscillation Index variability conformed to a combination of the variations of Darwin and Tahiti pressure. Over the El-Niño Southern Oscillation spectra, the Darwin pressure shared variations associated with the SSN tendency while the Tahiti had a connection with the stratospheric quasi-biennial oscillation modulating annual cycle. The power peak near the 3.5-year period comprised the third harmonic of the sun and the second of the modulated annual cycle. The derived harmonics came from both sources, so the initiation of El-Niño could be predicted more successfully when including the effects of the sun and QBO.

Key words: SOI, QBO, ENSO, SSN, modulation, spread spectrum

1. Introduction

Up to the present time, many authors have discussed the solar cycle effects on weather formation. They considered the small variability in the luminosity resulting from sunspot variation over a short period of less than a century. Most of the authors concluded that there were no meaningful effects of the sun on the atmospheric circulation (Moore et al., 2006). This conclusion may be acceptable when only a linear relationship between the sun and atmospheric motions is being sought. Some findings in the above trail have been successful for the stratosphere (Labitzke and van Loon, 1993) and the troposphere (Lim et al., 2006).

All of the models employed to explain the El-Niño system primarily used the ocean surface temperature and atmosphere parameters without the explicit cooperation of the sunspot numbers (SSNs) and the quasi-biennial oscillation (QBO). The previous two effects would have been included implicitly in the comprehensive models. Explicit mechanisms to reflect the phenomena and their modulation involved in the atmospheric motions did not exist for the simple models, even for the coupled ocean-atmosphere models (Jin et al., 2008). Many researchers of the El-Niño Southern Oscillation (ENSO) concentrated on the internal dynamics of the coupled ocean and atmosphere system (Sheinbaum, 2003).

Many meteorologists were reluctant to accept the frequency change that was probably brought on by the modulation of the atmosphere motions by a regular forcing. However, the frequency shift was common due to its strong nonlinearity in nature and thus a drastically different viewpoint might be admissible. The nonlinearity in atmospheric motions meant that linear treatment of the frequency components was inherently restricted to assess the reality of the motions.

Unfortunately, no proper analytical methods dealt with the nonlinearity of the atmospheric motions. Spectrum and correlation analyses were essentially linear. Even though the available methods had unavoidable deficiencies, we carefully traced seemingly fundamental frequencies and their modulation and derived harmonics. For clarity, we concentrated on the transfer of power in the frequency and phase relationship between the frequency peaks appeared in the spectrum functions as well as the correlation peaks in the autocorrelation

*Corresponding Author: G.-H. Lim, School of Earth and Environmental Sciences, College of Natural Sciences, Seoul National University, Gwanak-ro 1, F47 R201, Seoul 151-747, Korea.
Phone : +82-2-880-6725, Fax : +82-2-887-4890
E-mail : gyuholim@snu.ac.kr

functions.

Although the Southern Oscillation Index (SOI) is a good indicator to diagnose the ENSO phenomenon, the index does not seem to contain the period of only one physical process. In other words, the SOI has a very broad spectrum and, furthermore, double peaks rather than one representative peak in its spectrum band (Torrence and Campo, 1998).

The SOI was defined by using the surface pressure values at two stations: Darwin and Tahiti. Then, we questioned whether or not the two pressure time series shared a common variation source. Is it reasonable to say that the broad frequency range of the SOI is natural although it represents the well-defined ENSO phenomenon only? We prefer as the answer “no”.

In the following section, the data sources were described, and we discussed the pertinence of the selected data sets for this study in Sections 2 and 3. In Sections 4 and 5, the autocorrelation function and the associated spectrum function were used for the analysis of the time series of the pressure values as well as the SOI index. The time evolution of power in the frequency domain was examined by using wavelet power spectrum. The conclusions are in Section 6.

2. Data

The data sets used for the analysis were the SOI and monthly values of the surface pressure at Darwin and Tahiti. We downloaded them from the website: http://www.bom.gov.au/climate that is managed by the Bureau of Meteorology of the Australian Government. The SOI index was based on the mean and standard deviation over the period of years from 1933 to 1992.

We obtained the SSNs and the stratospheric QBO index from the National Aeronautics and Space Administration and the National Centers for Environmental Protection of the USA, respectively. The SSN is the International sunspot numbers, and the QBO index was defined with the zonal average winds at the 30 hPa level at the equator. We used the SSN data for a period of 138 years (1876~2013) to match the SOI and pressure values in the time domain. The QBO index covered 66 years from 1948 to 2013.

All of the data sets comprised monthly values. They were well documented by the accredited agencies around the world and many authors examined the data exhaustively. The data sets were free from errors and reliable in their quality. There were diverse results derived from the data sets.

3. Global analysis

3.1 Time domain analysis

In Fig. 1, the time series of the SOI, Darwin, and Tahiti showed a feature of random noise. The feature somewhat contradicted the considerable magnitude of the one-point lag correlations of 0.63, 0.50, and 0.484 for the SOI, Darwin, and Tahiti, respectively. Their irregularity in time strongly contrasts with the SSN and QBO oscillations. The noisy feature was even clearer in the autocorrelation functions. Overall, the three autocorrelation functions show 2~3 years of oscillation, which primarily reflected the effects of the QBO.

At a lag of 28 months marked with the thick blue bars in the ACFs of Fig. 1, there is no positive correlation at all for Tahiti pressure (Fig. 1f). Such a deviation may originate from the weakening of the QBO frequency due to a modulation style interaction. The estimated modulation periods were 84 months (or 7.0 years) and approximately 6.5 months. The periods were obtained by calculating the modulation frequency of the following two components: the annual period of 12 months and the 14 months period that was half of the 28 months QBO period. The reason of having 14 months instead of 28 months will be discussed in Section 3.2. The resulted short period of 6.46 months from the modulation may be smeared with other high frequency components. We are more interested in the 84 months period from the modulation.

In Figs. 1d and 1f, the autocorrelation peak related to the SSN was more pronounced at Darwin and the QBO effects were stronger at Tahiti. The SOI comprised the both, which signified that it was illogical to say that the SOI reflected only one physical process, even though it was pertinent to represent the intensity of ENSO to a certain degree (Trenberth, 1984).

We expected a bilateral interaction of the QBO with the tropical convections resulted from the ENSO activity. However, we like to accept the former modulation of the latter from the fact that the QBO preceded two months the SOI in the cross-correlation function (not shown).

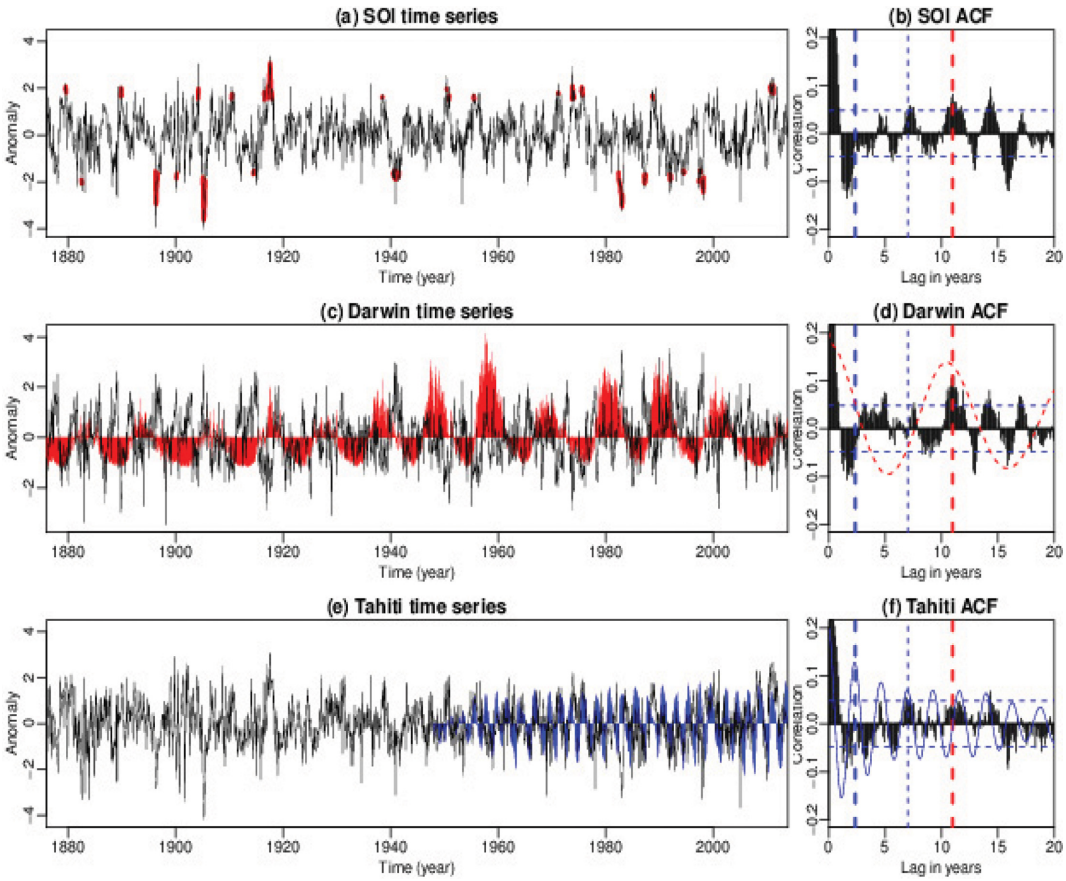

Fig. 1. (a, c, e) Pressure time series and (b, d, f) autocorrelation functions. (a, b) are for the SOI, (c, d) for Darwin, and (e, f) for Tahiti. The red blobs in (a) marked the smoothed SOI values exceeding 1.5 in a unit of standard deviation. The smoothing was carried out by applying a 1-2-1 filter two times. The red shading in (c) shows the smoothed time series of SSN produced by applying the 1-2-1 filter five times and the autocorrelation of the raw SSN with dashed curve in (d). The blue shading in (e) shows the QBO time series and its autocorrelation with the blue dashed in (f). For comparison, we scaled down both of the autocorrelations by one-fifth. The dashed red bar marked a lag of 11 years and the thick blue a lag of 28 months. The thin blue bar locates a lag of 84 months or 7 years. The horizontal dashed lines denote a 5% significance level for the correlation.

The Darwin pressure responded to the forcing of the SSN for the short time span centered at a lag of 11 years. For the other lag times, it was difficult to designate similarity between the correlation functions of Darwin and the SSN (Fig. 1d). Such a localized correlation peak at a certain lag time appeared as power peaks at the integer multiples of the primary frequency in the corresponding spectrum function.

By considering the simultaneous effects of the sun and the QBO on the pressure change at the Darwin and Tahiti, we constructed scatter diagrams between the SOI and SSN and between "aSOI" and the QBO index for different values of SSN and QBO and displayed them in Fig. 2. We adopted a word "aSOI" to designate the orthogonal component to the SOI. The "aSOI" is the same as the quantity described as noise by Trenberth (1984). The crossed statistics for the above mentions parameters are given in Fig. 3. The both figures clearly show the contrasting features in the parallel and cross relationships between the SOI (aSOI) and the SSN (QBO).

During the most rapid decrease phase of SSN, SOI had a negative maximum value in Fig. 2a, even clearer in Fig. 2b. The SOI minima period accompanied high pressure at Darwin and low pressure at Tahiti. The level of correlation was high for the transition phases

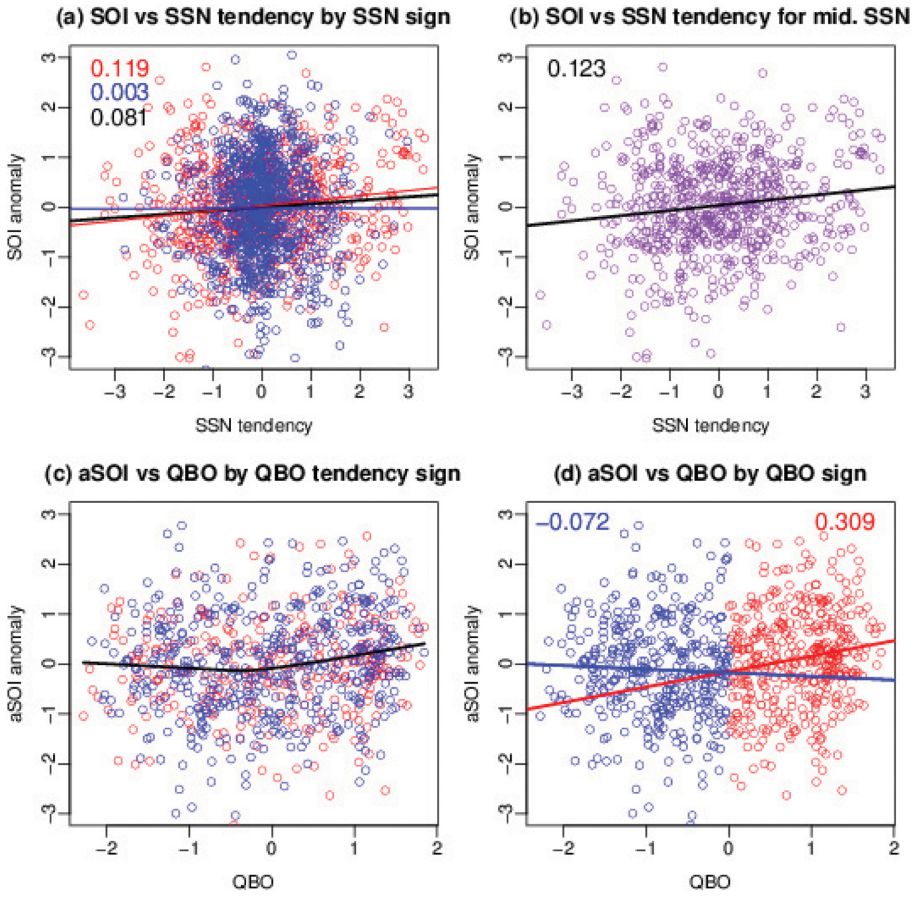

Fig. 2. Scatter diagrams of the SOI versus the SSN tendency (a, b) and "aSOI" against the QBO index (c, d) for the different categories of parameters. (a) SOI versus the SSN tendency by the positive (686 red dots) and negative (970 blue dots) values of SSN. Color coded linear fits had correlation coefficients of 0.119, 0.003, and 0.081 for the entire pairs. (b) SOI versus the SSN tendency for the values of SSN from −0.005 through 3.0 with a linear fit in black. The obtained correlation coefficient 0.123 for 678 pairs was significant at least 5% based on the null hypothesis. (c) "aSOI" against QBO for the positive tendency (403 red dots) and negative tendency (389 blue dots) of the QBO. The nonlinear fit in black was for the entire 792 pairs. (d) As for (c) but for the different signs of the QBO. The magnitudes of SOI were marked as a function of QBO for the positive values (306 red dots) and the negative values (489 blue dots) of QBO. The corresponding linear fits had the correlation coefficients 0.309 and −0.072 in order. For analysis, the moving averages of SOI, "aSOI", QBO, and the SSN tendency were produced by applying the 1-2-1 filter five times. The term "aSOI" means "not SOI" component, which is the averages of Darwin and Tahiti pressure anomalies.

and with large values of SSN. Overall, the negative phase of SSN tendency favored the El-Niño condition (Fig. 2b). The relationship was consistent with the increase of convective motions by the evaporation of liquid water from the ocean surface rather than by direct warming of the sea surface due to the sun light (Lim et al., 2006).

From Figs. 2c and 2d, the relationship of "aSOI" to QBO did not show any dependency on the QBO tendency but had a clear dependency to the sign of QBO, in other words, to the direction of the wind. The above relationship implied the importance of convections than direct mechanical forcing of the QBO on the Walker circulation.

The dynamics inferred from Fig. 2 could not be ascribed to a chance originated from a stochastic process when considering the strong contrast between the features in Fig. 2 and a similar analysis but between

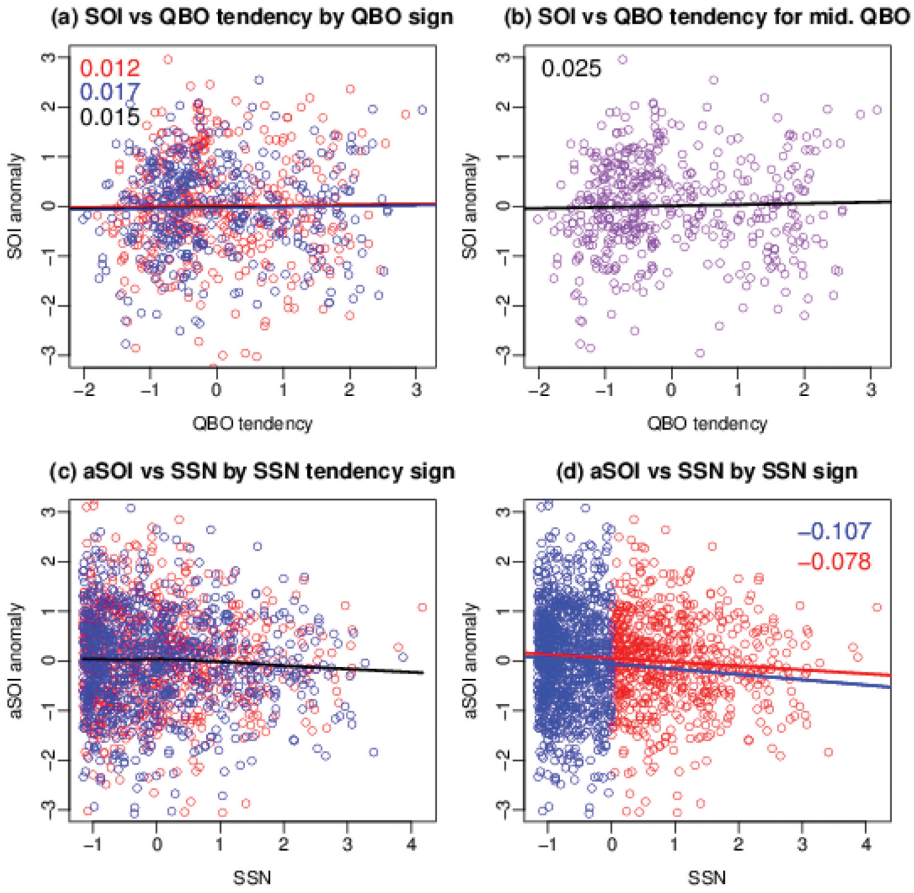

Fig. 3. As in Fig. 2, but for Scatter diagrams of the aSOI versus the SSN tendency (a, b) and "aSOI" against the SSN index (c, d) for the different categories of parameters.

SOI (aSOI) and QBO (SSN) shown in Fig. 3. The strong sun decreased the surface pressure at the both stations in general.

In Fig. 4, we were able to reconfirm the previous statistics inferred from Figs. 1, 2, and 3. The Fig. 4 showed the magnitude of SOI in the phase domain of SSN and SSN tendency. In this scatter diagrams, the distribution was noisy as consistent with the small correlation coefficients in the previous analysis. However, the features deviated from a uniform distribution in magnitude as well as position. The strong dissimilarity between Figs. 4a and 4b revealed the different mechanisms working on SOI and "aSOI", which could be interpreted as Darwin and Tahiti affected by the different forcing.

In Fig. 4a, the spatial density of the circles revealed the strong positive skewness of SSN time series. The SSN had a long dormant period and a short peak time in general. With less clarity, we could point out that positive SSN tendency side was populated with blue bubbles and the negative side with red ones. In Fig. 4b, the sparse and dense phases with bubbles coincided with the rapid downward movement of westerly and the slow downward of easterly, respectively. The positive QBO phase had more blues than the negative phase did. In the positive phase of the QBO index, we had high pressure anomaly at Tahiti and Darwin simultaneously.

3.2 Spectrum functions

For all of the spectrum functions in Fig. 5, the enhanced power appeared for a frequency band that ranged from the solar cycle at a low-frequency end to the QBO cycle at a high-frequency side. Over the

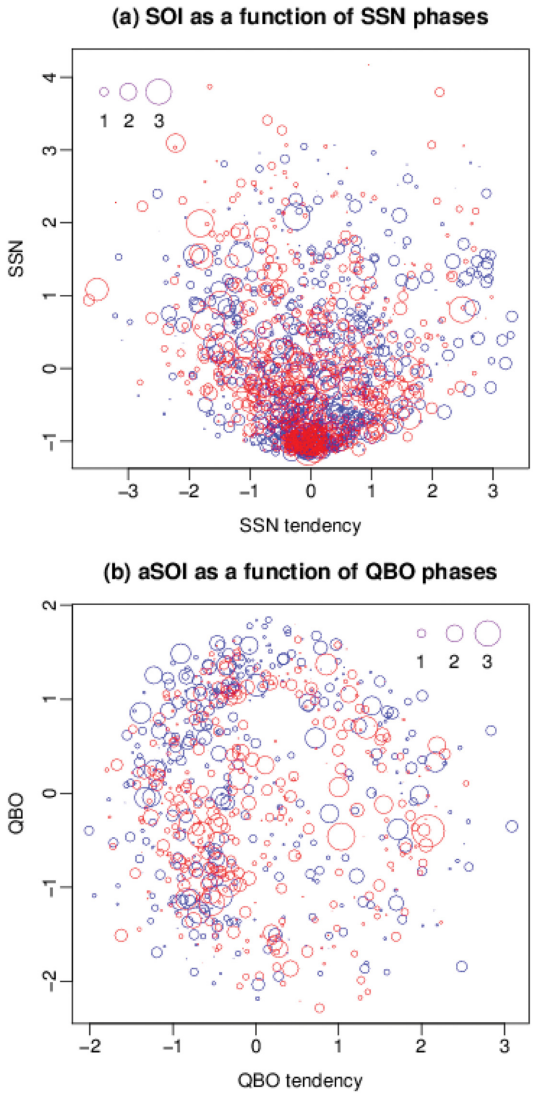

Fig. 4. Scatter diagrams of (a) SOI anomaly in the phase domain of SSN and the SSN tendency and (b) the "aSOI" anomaly against the values and tendency of the QBO index. The position and size of a circle represent the phase domain coordinates and magnitude. Red and blue denote positive and negative anomaly, respectively. The legend digit 1, 2, 3 means the multiplier of the standard deviation of the corresponding time series. The tendency was computed by taking difference of pressures at before and after a given time. We normalized the resulted series with its standard deviation.

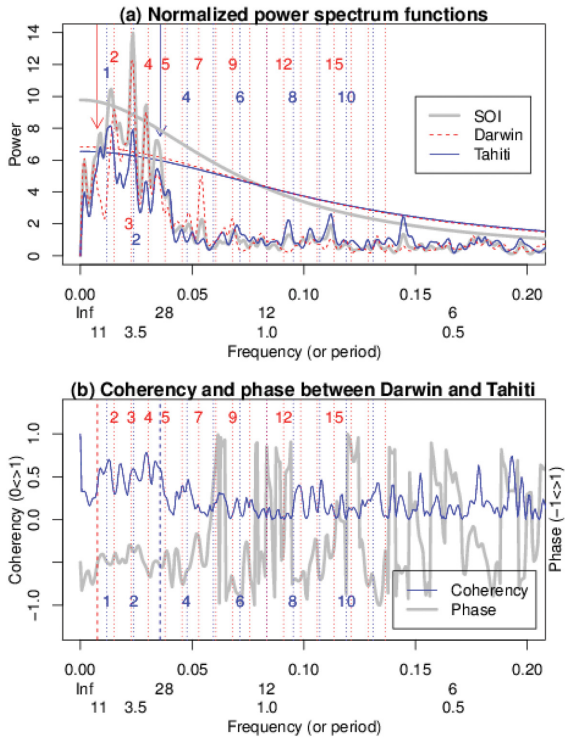

Fig. 5. (a) Power and (b) cross spectra as a function of frequency. The SOI, Darwin, and Tahiti spectra are in grey, red, and blue curves, respectively. The spectrum functions were smoothed by applying a 1-2-1 filter five times. The smooth curves in grey, red, and blue mark a 5% significance against the red noises. All of the spectrum functions were normalized to have a unit magnitude at each frequency for the case of average. The SSN and QBO frequencies were marked with the downward red and blue arrows in (a) and with respective dashed bars in (b). The red and blue digits for the dotted lines were the harmonic numbers of the two basic periodicities of 132 months (11 years) related to the SSN and 84 months of the QBO-modulating annual cycle. Phase values were divided by π.

frequency band, the most pronounced peak appeared at 3.5 years, which was close to the third harmonic of the sun with a 3.7 year period and coincided with the second harmonic of QBO-modulating annual cycle with a period of 3.5 years that was equal to 2/84 in a unit of cycle/month. The 84 month was the period of the primary frequency of the QBO-modulating annual cycle.

At high frequencies shorter than the QBO period of 28 months, a statistically significant peak did not exist, except for the SSN component with the 18-month period for the Darwin pressure only. Over the band with enhanced power, the overall coherency was 0.5 compared with the value of nearly zero for the high-

frequency components. The shape of the spectrum functions deviated from the air temperature variation that was used for environmental influences and suitably described as red, brown, or black noise by Cuddington and Yodzis (1999) and Halley and Kunin (1999).

In the phase domain, the Darwin maximum pressure led the Tahiti minimum pressure by about 90 degrees rather than 180 degrees. The fact apparently contradicted the same 3-year lag between the Darwin and Tahiti pressure values with respect to the SSN and the almost simultaneous peaks of pressure with respect to the QBO by two-month delay only. The essential reason for such differences may arise from the combination of the results for the both periods simultaneously.

The Darwin pressure series had power peaks at 66 months (5.5 years) and 44 months (3.7 years). The periods were the harmonics of the primary 11-year period. In Fig. 5a, the power of the fundamental frequency was small compared with those of the second and the third harmonics. The harmonics might have originated from the strong nonlinear and indirect response of the surface pressure to the sun's variation in intensity. The exact mechanism of amplification of a certain harmonic is beyond the object of this work.

The weak 11-year frequency peak in the spectra did not imply an absence of effects from the sun's activity. For the nonlinear systems, the power of the forcing frequency could be transferred to its harmonics. The transfer was possible due to a spread spectrum style modulation (Barnston, 1982).

Maximum and minimum pressure values appeared at the period with the largest SSN tendency instead at the period of extreme values of SSN. When the SSN decreased rapidly, the Darwin pressure reached the highest value and the lowest pressure appeared at Tahiti. The Darwin pressure was proportional to the SSN value three years before. Such a relationship suggests that the tendency of SSN may be directly connected to the magnitude of the pressure anomalies at the both stations, which was discernable in Figs. 2a and 2b.

The Tahiti pressure showed a more wavelike response than the Darwin pressure. The shape was apt to produce the 7-year frequency peak by the QBO modulation of the annual cycle. The 7-year harmonics were possible when considering the surface pressure dependencies on the states of the QBO, together with the lowest pressures at the transition state of the QBO winds (Figs. 2c and 2d). More specifically, the annual cycle produced the 84-month period, while interacting with the QBO in the time scale of its half time instead of its full 28 months. The best fitting curve in Fig. 2c was based on the method by Cleveland (1979).

3.3 Spread spectrum modulation

To our knowledge, no one has investigated the outputs from the modulation of random time series with a sinusoidal function in time. It is worthwhile to examine the outputs from such a modulation or interaction. In atmospheric motions, the convections may be considered as stochastic processes when comparing with the large-scale motions. The latent heat is the second most important energy source after solar heating for the circulation of the atmosphere. We also have to remember that the latent heat also came from solar radiation.

For an illustration, let us assume a time series of random numbers multiplied by a cosine function of time. The latter could simulate an almost regular cycle such as the SSN. An ideal white noise process can be written by assuming a unit amplitude with an infinite number of frequencies. By considering the Fourier transform of a random process, we are able to express a modulated time series as follows:

$$M(t) = A\cos(2\pi f_0 t)\cdot B\Sigma_{f_k=-\infty}^{+\infty}[\cos(2\pi f_k t) + \sin(2\pi f_k t)].$$

The summation represents the assumed white noise process. A and B denote the amplitudes of the forcing and the forced processes, respectively. The amplitudes A and B did not significantly affect the final output of modulation. The modulation can produce a new frequency set as follows:

$$M(t) = \frac{AB}{2}\Sigma_{f_k=-\infty}^{+\infty}[\cos\{2\pi(f_k \pm f_0)t\} + \sin\{2\pi(f_k \pm f_0)t\}].$$

The modulated frequency is as follows:

$$f_{mod} = f_k \pm f_0.$$

No power of frequency zero (0.0) decreased by half the power of the forcing frequency in the spectrum of the modulated time series. The power of the forcing frequency moved by half to the adjacent frequencies separated by f_0. At the same time, the displaced power of the frequency was compensated for by the powers from the adjacent frequencies. All of the frequencies, except for f_0, released and regained equal

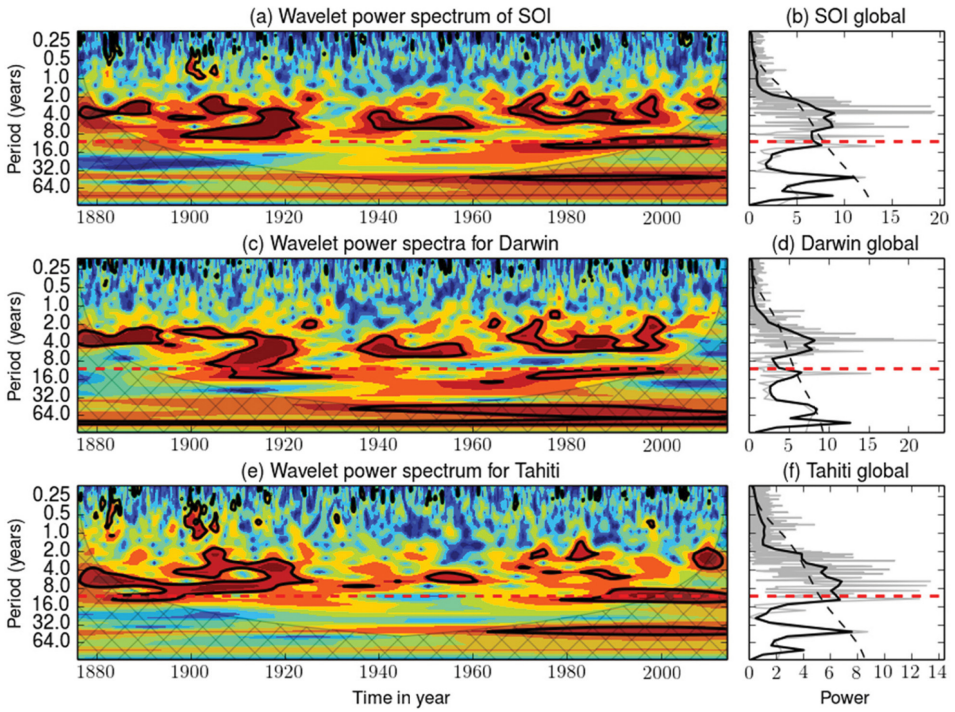

Fig. 6. Wavelet power spectra (a, c, e) and the corresponding global spectra (b, d, f) of the SOI, Darwin, and Tahiti pressure anomalies. A significance level of 5% was marked by the thick contours in the left-hand side Figs. and the dashed curves in the right. The highly fluctuating grey curves in the right-hand side are the raw spectrum from the Fourier transform. The red-dashed lines mark the 11-year period.

amounts of power, so the modulation did not change the power of each frequency. The only exception was for the forcing frequency. The above simple and lucid model supported the disappearance of the power of the forcing frequency after modulation. Lim et al. (2014) detailed the characteristics of this type of modulation and successfully reproduced the previous theoretical prediction in their countless numerical experiments. On the other hand, the enhancement of the derived harmonics were yet unresolved and conceived as caused by a unique regime of the pressure variation at the two stations.

3.4 Effects of the SSN and QBO

The high pressure at Darwin and low pressure at Tahiti appeared frequently for the period after three years from the maxima of the SSN. The time lag relationship resulted in the almost simultaneous linear relationship between the SOI index and the SSN tendency. Development of convective motions over the tropics might be affected by the time rate of change of SSN combined with the surface temperature changes of diverse time scales. The changes came from an annual cycle, the diurnal variation, and other various mechanism. The convective motions were mostly controlled by the available amount of water vapor and the stability of the atmosphere that had a strong connection with the heat capacity of the concerned region.

In a relative sense, Tahiti was in aqua world with large heat capacity. On the other hand, Darwin experienced dry climate with a small heat capacity due to the influences of the continents of Asia, Australia, and the Maritime Continent. During the phase of negative SSN tendency, Darwin could cool down much faster than Tahiti did. The fact suggested more stable atmospheric condition in the region of Darwin than of Tahiti. To the contrary, warm and water abundant Tahiti area would have stronger convective motions in the decreasing phase of SSN. During the period of a positive SSN tendency, we expected more frequent La-Niña situation.

The pressure increased at the both stations for the positive and negative extreme phases of the QBO. In Fig. 2c, the low pressure coincided with the null wind phase of the QBO. The relationship could be explained by considering the water vapor increase and the more active convection at this time of phase (Lim et al., 2008). The pressure changes were nearly independent of the time rate of change of QBO or its tendency, as evident from Fig. 2a.

The Coriolis force could be responsible for the asymmetrical response of the pressure to the westerly and easterly phases of the QBO. Due to the Coriolis deflection, the westerly converged toward the equator and the easterly diverged away from the equator meridionally. The convergence or divergence could suppress or enhance the convective motions over the tropics (Collimore et al., 1998; Lim et al., 2008). Over the tropics, the weak convective motions or less rainfall events resulted in high pressure at the surface.

4. Wavelet analysis

From the wavelet power given in Fig. 6, we can point out that a 3.5 year period was dominant for Darwin and a 7.0-year period for Tahiti in the temporal variation of pressure. The SOI power had a similar shape that resulted from the addition of the powers of Darwin and Tahiti. Such a relationship held for the entire period of data. The relationship suggested that the SOI spectrum power was interpretable as the combined power of both of the stations. The feature reflected the definition of SOI.

As consistent with the global spectra discussed in the previous section, we also designated the 3.5-year and 7.0-year frequencies of the power peak and the pronounced suppression in the global wavelet spectrum and the spectrum functions without smoothing. We marked 5% significance level for wavelet analysis (Cazelles et al., 2014)

From the cross wavelet analysis of Tahiti and Darwin, the periods with high coherency showed nearly opposite or antipodal relationships (not shown). The feature suggests a well-defined Walker circulation; the opposite pressure anomalies at the two stations. For the other times, a weak relationship resulted in the loss of coupling between the convective motions at the two stations and an ambiguous phase relationship between the pressure changes at the two stations.

5. Conclusions

The power spectra of the SOI and the Darwin and Tahiti pressures resembled a band-wisely enhanced white noise process. The elevated power was resolved for the frequency band ranging from the SSN period to the QBO period. The other frequency band had a weak and constant power over the frequencies (Fig. 5).

The most pronounced frequency of the SOI, of which period was 3.5 years, comprised the components of the third harmonic of the SSN and the second one of the QBO-modulating annual cycle. The primary forcing frequency might have less power than its harmonics when the spread spectrum type modulation occurred with a proper spectrum broadening. The exact process should be sought in future.

The periods of positive and negative tendency of SSN, which coincided with increase and decrease phases of the SSN showed the pressure values at the two stations for the conditions of the El-Niño and La-Niña, respectively. The phase with the strongest negative tendency of SSN coincided with the periods of maximum pressure at Darwin and the minima at Tahiti. On average, the highest peak values of SSN appeared by about three years before the minimum tendency period for which SSN decreased most rapidly (Fig. 2b). No signature of the maxima or minima of the SSN appeared at the times of high or low-pressure values at the two stations.

The QBO controlled the sea level pressure of the two stations in the same fashion, which was in striking contrast to the sun's effects. By referring the QBO cycle, null winds decreased the pressure and the westerly favored the highest pressure and the easterly the next highest pressure at both of the stations. The features were understandable by considering the effects of the wind shear in the vertical direction on the convections over the tropics, and the meridional convergence and divergence by the Coriolis force.

The proposed explanation complements the role of the atmosphere in the development of El-Niño in its present initiation theory, which started with the anomalous weakening of the easterly trades. Based on our findings, the forecasting skill of El-Niño could improve by including QBO and SSN variability in cooperation with the traditional methods reflecting the state of the ocean.

Acknowledgments

This work was funded by the Korea Meteorological Administration Research and Development Program under Grant KMIPA2015-5090. The authors were also supported by the second stage of the Brain Korea 21 Project.

REFERENCES

Baldwin, M. P., and Coauthors, 2001: THE QUASI-BIENNIAL OSCILLATION. *Rev. Geophys.*, **39**, 179-229.

Cazelles, B., K. Cazelles, and M. Chevez, 2014: Wavelet analysis in ecology and epidemiology: impact of statistical tests. *J. Roy. Soc. Interface*, **11**, 20130585, http://dx.doi.org/10.1098/rsif.013.0585.

Cleveland, W. S., 1979: Robust locally weighted regression and smoothing scatterplots. *J. Am. Stat. Assoc.*, **74**, 829-836.

Collimore, C. C., M. H., Hitchman, and D. W. Martin, 1998: Is there a quasi-biennial oscillation in tropical deep convection?. *Geophys. Res. Lett*., **25**, 333-336.

Cuddington, K. M., and P. Yodzis, 1999: Black noise and population persistence. *Proc. R. Soc. Lond. B* 1999, **266**, doi:10.1098/rspb.1999.0731.

Halley, J. M., and W. E. Kunin, 1999: Extinction Risk and the 1/f Family of Noise Models. *Theor. Popul. Biol.*, **56**, 215-230.

Jin, E. K., and Coauthors, 2008: Current status of ENSO prediction skill in coupled ocean-atmosphere models. *Clim. Dynam.*, doi:10.1007/s00382-008-0397-3.

Labitzke, K., and H. van Loon, 1993: Some recent studies of probable connections between solar and atmospheric variability. *Ann. Geophys*., **11**, 1084-1094.

Lim, G.-H., Y.-C. Suh, and B.-M. Kim, 2006: On the origin of the tropical atlantic decadal oscillation based on the analysis of the ICOADS. *Quart. J. Roy. Meteor. Soc*., **132**, 1139-1152.

_____, A.-S. Suh, and Y.-C. Suh, 2014: Variability of the annual amounts of station precipitation revealed by autocorrelation functions and power spectra. *Proceedings ITISE 2014 International work-conference on Time Series*, Granada, June, 25-27 2014, **1**, 15-27.

_____, Taehyon Shim, A.-S. Suh, D.-L. Lee, and W. Choi, 2008: The characteristics of the band-pass filtered time series of the zonal averages of monthly mean values based on ERA-40 reanalysis. *Atmos. Sci. Lett.*, **9**, 134-139.

Moore, J., A. Grinsted, and S. Jevrejeva, 2006: Is there evidence for sunspot forcing of climate at multi-year and decadal periods?. *Geophys. Res. Lett*., **33**, L17705, doi:10.1029/2006GL026501.

Pickholtz, R. L., D. L. Schilling, and L. B. Milstein, 1982: Theory of spread-spectrum communications-A tutorial. *IEEE Trans. Commun*., **COM30**, 855-884.

Sheinbaum, J., 2003: Current theories on El Niño-Southern Oscillation: A review. *Geofís. Int.*, **42**, 291-305.

Torrence, C., and G. P. Compo, 1998: A practical guide to wavelet analysis. *Bull. Amer. Meteor. Soc.*, **79**, 61-78.

Trenberth, K. E., 1984: Signal versus Noise in the Southern Oscillation. *Mon. Wea. Rev*., **112**, 326-332.